RSC Publishing Dalton Transactions

Bromide ion binding by a dinuclear gold(I) N-heterocyclic carbene complex: A spectrofluorescence and X-ray absorption spectroscopic study

Journal:	*Dalton Transactions*
Manuscript ID:	DT-ART-08-2012-031817.R2
Article Type:	Paper
Date Submitted by the Author:	n/a

Complete List of Authors:	Berners-Price, Sue; Griffith University, Institute for Glycomics Wedlock, Louise; University of Western Australia, ; Griffith University, Institute for Glycomics Aitken, Jade; The University of Sydney, School of Chemistry; Australian Synchrotron, ; KEK, Institute of Materials Structure Science Barnard , Peter; La Trobe University, Department of Chemistry

Cite this: DOI: 10.1039/c0xx00000x

www.rsc.org/xxxxxx

ARTICLE TYPE

Bromide ion binding by a dinuclear gold(I) *N*-heterocyclic carbene complex: A spectrofluorescence and X-ray absorption spectroscopic study

Louise E. Wedlock,[a,b] Jade B. Aitken,[c] Susan J. Berners-Price*[a,b] and Peter J. Barnard*[d]

Received (in XXX, XXX) Xth XXXXXXXXX 200X, Accepted Xth XXXXXXXXX 200X
DOI: 10.1039/b000000x

Fluorescence and X-ray absorption spectroscopy were used to investigate the anion binding properties of a luminescent, dinuclear Au(I) *N*-heterocyclic carbene (NHC) complex ($[\mathbf{1}]^{2+}$) with a short Au(I)•••Au(I) contact. The addition of Br^- ions to a DMSO solution of $[\mathbf{1}](PF_6)_2$ caused a red-shift in the fluorescence emission band from 396 nm to 496 nm. Similarly, the addition of Br^- ions to $[\mathbf{1}](PF_6)_2$ caused a decrease in the energy of the Au L_3-edge in the X-ray absorption spectrum, consistent with the formation of an association complex between the cation $[\mathbf{1}]^{2+}$ and Br^- ions. Solution-based structural studies of the association complex were carried out using extended X-ray absorption fine structure (EXAFS) modelling of the Au(I)•••Au(I) core of the cation. These studies indicate that the association complex results from Au(I)•••Br^- interactions, with the Br^- ions occupying two partially occupied sites at ~2.9 and 3.9 Å from the Au(I) atoms.

Introduction

For many years the attractive (aurophilic) interaction between closed shell Au(I) centres has received considerable interest from the scientific community.[1, 2] For linear two-coordinate gold complexes, in the +1 oxidation state, sub Van der Waals Au(I)•••Au(I) contacts of less than 3.4 Å are widely observed. These attractive interactions have been estimated to have similar energies to those of standard hydrogen bonds, ~ 20 – 40 kcal mol^{-1}.[1] Aurophilic interactions are often observed in the solid state for Au(I) compounds, and they have been deliberately employed in the synthesis of polynuclear Au(I) complexes.[3] In addition to the influence of aurophilicity on the structural chemistry of Au(I), this phenomena is commonly associated with intriguing photophysical properties, such as luminescence emission with large Stoke's shifts.[4] The luminescent properties associated with dinuclear Au(I) systems has made them an important family of luminescent metal complexes.[5]

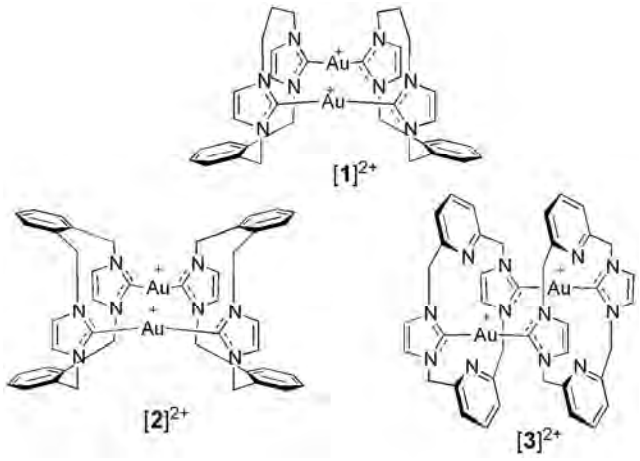

Chart 1 Previously reported dinuclear Au(I) *N*-heterocyclic carbene complexes with bridging cyclophane ligands.

A series of dinuclear Au(I) *N*-heterocyclic carbene (NHC) complexes, in which the two Au(I) ions are supported by bridging cyclophane ligands (for example, $[\mathbf{1}]^{2+}$ – $[\mathbf{3}]^{2+}$, Chart 1) have been previously described.[6, 7] These compounds show potential as luminescent probes, and the intracellular distribution of $[\mathbf{1}]^{2+}$ (as a bromide salt) has been mapped inside live cancer cells by confocal fluorescence microscopy.[7] Structural studies showed that the cyclophane ligand framework allows the Au(I)•••Au(I) distance to be precisely modulated. For example cations $[\mathbf{1}]^{2+}$ and $[\mathbf{2}]^{2+}$, have Au(I)•••Au(I) contacts of 2.93[7] and 3.05 Å,[6] respectively, (< 3.4 Å – suggestive of an aurophilic interaction), and both complexes exhibited intense solution luminescent behaviour. In contrast, complex $[\mathbf{3}]^{2+}$ displayed a longer

[a] *Institute for Glycomics, Griffith University, Gold Coast Campus, QLD 4222, Australia. Tel: +61 7 3735 7290, E-mail: s.berners-price@griffith.edu.au;*
[b] *School of Chemistry and Biochemistry, University of Western Australia, 35 Stirling Highway, Crawley, WA 6009, Australia.*
[c] *School of Chemistry, The University of Sydney, NSW, 2006, Australia; Australian Synchrotron, Clayton, Victoria, 3168, Australia; Institute of Materials Structure Science, KEK, Tsukuba, Ibaraki 305-0801, Japan.*
[d] *Department of Chemistry, La Trobe Institute of Molecular Science, La Trobe University, Bundoora, VIC 3086, Australia. Tel: +61 3 94792516; Email: p.barnard@latrobe.edu.au;*
† Electronic Supplementary Information (ESI) available: Table S1: Constraints and restraints used in the MS EXAFS analysis of 1.$(PF_6)_2$ in DMSO; Table S2: Paths and importance factors for the MS refinement of the EXAFS of ***1***.$(PF_6)_2$. ^{1}*H NMR spectrum for* ***[1]***$(PF_6)_2$. *See DOI: 10.1039/b000000x/*

Au(I)•••Au(I) distance (3.76 Å) and was not luminescent. In these studies, a qualitative relationship was also demonstrated between the emission profile and the Au(I)•••Au(I) distance, e.g. with shorter Au(I)•••Au(I) distance associated with red-shift in emission energy.

It was previously noted that the emissive behaviour of $[\mathbf{1}]^{2+}$ is significantly influenced by the chosen solvent, and on the nature of the counter anions.[7] Other groups have demonstrated that the influence of 'outer sphere ligands' e.g. solvent or the counterion, can significantly influence the fluorescence emissive behaviour of complexes with short Au(I)•••Au(I) contacts,[8-12] leading to fascinating solvochromic, vapochromic and anion-dependent behaviour.[12, 13] Results obtained by Che and co-workers show that the metal-centred emission from the the excited state of dinuclear Au(I) complexes with bridging phosphine ligands occurs in the UV region,[9, 14] and that this emission is red-shifted for exciplexes formed by the associated of weakly coordinating counterion or solvent molecules to the Au(I) centres.[9, 11] These workers assigned the excitation of the dinuclear Au(I) complexes displaying aurophilic interactions to the $5d\sigma^* \rightarrow 6p\sigma$ transition, producing the $^3[d\sigma^*p\sigma]$ excited state.[8-11] This excited state electron configuration represents a formal Au(I)-Au(I) single bond and the visible emission resulting from exciplexes of the form $[Au_2(dcpm)_2]Y_2$ (Y = a range of anions, including halides, and dcpm = bis(dicyclohexylphosphino)methane) originates from the $^3[d\sigma^*p\sigma]$ excited-state, which is perturbed by anion/solvent association.[8, 9, 15]

Solution based structural studies for dinuclear Au(I) complexes which display aurophilic interactions are rare. In one report, the Au(I)•••Au(I) separation and solvent / anion•••Au(I) interaction were studied for a series of dinuclear Au(I) complexes bearing diphenyl diphosphinomethane, μ-xantphos and μ-dpephos ligands, using EXAFS (extended X-ray absorption fine structure).[16] X-ray absorption spectroscopy (XAS) and EXAFS provides an excellent method for probing the coordination sphere surrounding the close Au(I)•••Au(I) contacts in solution, and in this paper we present our results for a combined fluorescence and X-ray absorption spectroscopic investigation of the influence of bromide counter ions on the fluorescence emission spectra of the dinuclear Au(I)-NHC complex $[\mathbf{1}]^{2+}$.

Experimental

Preparation of the Au(I) complex, [1](PF$_6$)$_2$

$[\mathbf{1}]Br_2$ was prepared and resolved into its *cis*- and *trans* diastereoisomeric forms by fractional crystalisation as reported previously.[7] The *cis*- diasterisomeric form of $[\mathbf{1}]^{2+}$ was used in all studies reported here. $[\mathbf{1}](PF_6)_2$: To a solution of $[\mathbf{1}]Br_2$ (0.4 g, 0.36 mmol) in hot water (10 mL) was added a filtered saturated aqueous solution of KPF_6 (15 mL).The pale green precipitate which formed immediately was collected by vacuum filtration and washed with water and methanol. Yield (0.3 g, 68 %) ^{1}H NMR (d_6-DMSO): δ 2.37-2.41 (m, br, 2H, $^2J_{HH}$ = 14.0 Hz, $N(CH_2)_2CH_2$), 2.65-2.73 (m, 2H, $N(CH_2)_2CH_2$), 4.45 (d, br, 4H, $^2J_{HH}$ = 14.0 Hz, $N(CH_2)_2CH_2$), 4.98 (dd, 4H, $^2J_{HH}$ = 14.0 Hz, $^3J_{HH}$ = 14.0 Hz $N(CH_2)_2CH_2$), 5.21 (d, 4H, $^2J_{HH}$ = 13.5 Hz, $ArCH_2$), 6.32 (d, 4H, $^2J_{HH}$ = 13.5 Hz, $ArCH_2$), 6.45 (d, br, $^2J_{HH}$ = 1.5 Hz, 4H, H_{imi}), 7.20 (s, br, $^2J_{HH}$ = 1.5 Hz, 4H, H_{imi}), 7.63-7.65 (m, 4H, H_{aryl}), 7.80-7.81 (m, 4H, H_{aryl}) ppm. ^{13}C NMR (d_6-DMSO): δ 29.4 ($N(CH_2)_2CH_2$), 51.1 ($N(CH_2)_2CH_2$), 52.5 ($ArCH_2$), 121.9 (C_{imi}), 122.4 (C_{imi}), 130.0 (C_{aryl}), 134.0 (C_{aryl}), 135.2 (C_q), 185.1 ($C_{carbene}$). Microanalysis: found : C, 32.5; H, 3.1; N, 8.9. $Au_2C_{34}H_{36}N_6(PF_6)_2 \cdot H_2O$ requires C, 32.4; H, 3.0; N, 8.9 %.

Spectroscopy

Nuclear magnetic resonance spectra were recorded on a Bruker AV-500 spectrometer (500.2 MHz for ^{1}H, 125.8 MHz for ^{13}C) and were internally referenced to solvent resonances. Fluorescence excitation and emission spectra were recorded on a Varian Cary Eclipse Fluorescence Spectrophotometer.

XAS experiments were performed at the Australian National Beamline Facility (ANBF), at beamline 20B at KEK, Photon Factory, Tsukuba, Japan. The beam was monochromated using a Si(111) monochromator, and harmonic rejection was performed by detuning the monochromator to 50%. The storage ring delivered a current of 250-400 mA at 3.5 GeV. All samples were contained in a generic sample holder with a 10 mm x 1 mm x 1 mm sample chamber filled with the sample and supported with Kapton tape windows. The samples were frozen in liquid N_2 before being placed into a helium cryostat (Cryodone REF-1577-D22) at ~ 13 K. Solution samples were prepared to a final concentration of 20 mM in DMSO. To investigate the influence of anions, a stoichiometric amount of tetrabutylammonium bromide solution (0.8 M in DMSO) was added to the DMSO solutions of $[\mathbf{1}](PF_6)_2$. The solutions were rapidly frozen as glasses plunging into a bath consisting of iso-pentane cooled to ~ -160 ºC with liquid N_2 before placing into the cryostat. A solid sample of $[\mathbf{1}]Br_2$ was prepared in boron nitride (BN) to give a final concentration of 10% w/w Au complex in BN.

A beam size of 3 mm x 1 mm was used to collect spectra in fluorescence mode at the Au L_3 edge (11919 keV, L_3 $2p_{3/2}$)[17] over a k range of 0 – 18 Å^{-1}, using Au foil as a standard against energy shifts in the monochromator.[17] A 36-element Ge detector was used to record between 3 and 6 scans.

XFIT Data Analysis

Multiple-scattering (MS) analyses of EXAFS data were performed using the XFIT suite of programs,[18, 19] which uses a non-linear least squares fitting of the EXAFS spectrum, through the minimisation of the sum of the square of the residuals. Model fitting calculations in XFIT were performed by the integration of the program FEFF6.01 which includes multiple scattering codes.[20, 21] The goodness of fit parameter R, and Monte Carlo calculations were performed as previously reported,[19, 20, 22, 23] and as described in the supporting information. The resulting r.m.s errors, from Monte Carlo analysis, were combined with systematic errors to obtain a final error estimate.[22] All background subtraction, splining and normalisation procedures were performed using XFIT as reported previously.[23]

A window from 1 – 16 Å^{-1} with a cosine edge function was applied to the EXAFS data. A window from 1.25 – 4.0 Å^{-1} was applied to the Fourier transform, which filtered the majority of the atomic EXAFS which is difficult to model (between 0 – 1.5 Å^{-1}).

EXAFS Model – Multiple Scattering (MS) Model

For the MS analysis of the EXAFS in the absence of any

anions, a fragment of the core of the cation $[\mathbf{1}]^{2+}$ was modelled, in three-dimensional space.[19] The model included two imidazolylidene rings on either side of the absorbing Au shell, and a second Au shell, orthogonal to the plane of the two heterocyclic rings (Fig. 1). The heterocyclic ring moieties were restrained to stay planar with respect to each other, as well as in the plane of the absorbing Au shell, but allowed to move towards or away from each other, thereby varying the Au-carbene distance during the fit. The intramolecular Au•••Au distance was allowed to vary in the direction perpendicular to the plane of the heterocyclic rings during the fit. A complete set of restraints and constraints for these models is contained in the Supporting Information (Table S1) where σ_{res} is analogous to the estimated standard deviation.

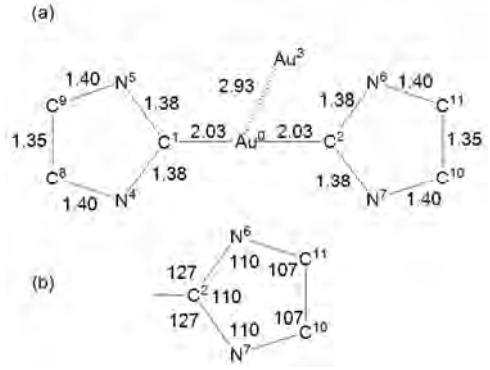

Fig. 1 Labelling of MS shells for the MS model used to fit the EXAFS of $[\mathbf{1}](PF_6)_2$ in DMSO at 13 K, showing a) the starting bond lengths (Å) and b) angles in the heterocyclic rings (º).

Results and Discussion

Consequences of anions on solution fluorescence behaviour

The emission spectrum (λ_{ex} = 313 nm) for a solution of $[\mathbf{1}](PF_6)_2$ in DMSO (0.2 mM) is shown in Fig. 2 (a) (λ_{em} = 396 nm). The excitation wavelength (λ_{ex} = 313 nm) corresponds to an absorption band in the UV-vis spectrum for $[\mathbf{1}]Br_2$.[7] As shown in Fig. 2 (b), the addition of Br^- (0 to 550 equivalents as tetrabutyl ammonium bromide) to the DMSO solution of $[\mathbf{1}](PF_6)_2$ results in a new emission band at 496 nm, with a concurrent decrease in the intensity of the band at 396 nm. An isosbestic point (*) is evident at approximately 465 nm. These results are consistent with the concentration dependent formation of an association complex between the $[\mathbf{1}]^{2+}$ cation and Br^- ions in solution. Here the emission at 396 nm may be assigned to the unassociated cation, while the emission band centred at 496 nm arises from an association complex, where Br- ions are bound to the Au(I) centres (Scheme 1).

Scheme 1 Equilibrium between the unbound cation $[\mathbf{1}]^{2+}$ and the association complex $[\mathbf{1}]Br_2$

It has been previously shown that for a dinuclear Au(I) complex with phosphine ligands, soft anions (e.g I^-), caused quenching of high energy emission (arising from the $^3[d\sigma^*p\sigma]$ excited state), with a simultaneous formation of a lower energy emission band.[8] Similar results are apparent in this study, with the high energy emission band (396 nm) decreasing in intensity as the Br^- concentration is increased. Concomitant with this is the appearance of a low energy emission band (496 nm), which appears likely to arise from an association complex formed between $[\mathbf{1}]^{2+}$ and Br^- ions. This is the first such study of the concentration-dependent equilibrium between Br^- ions and a dinuclear fluorescent NHC complex, and such intriguinging results prompted us to investigate the structure of this association complex, using X-ray absorption spectroscopy.

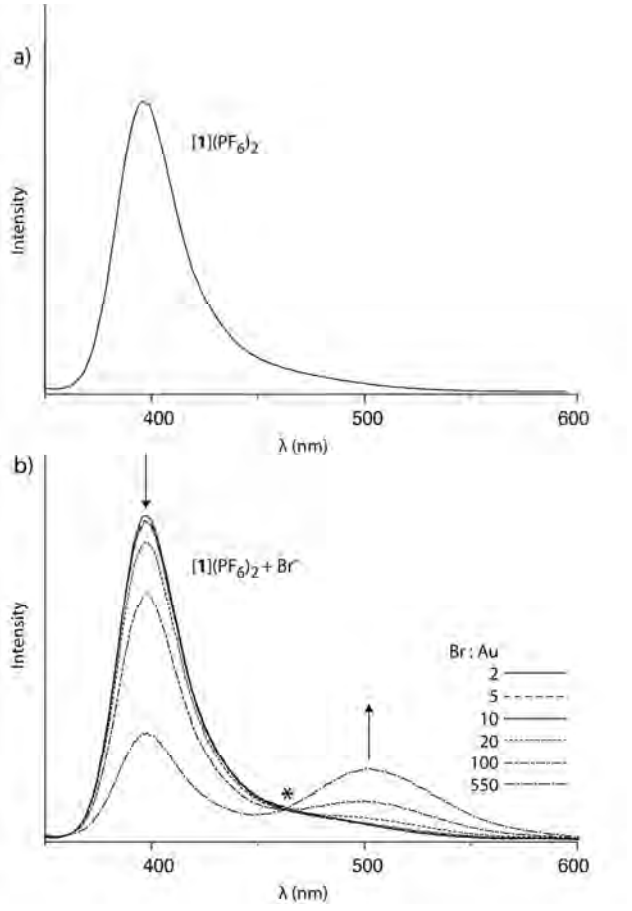

Fig. 2 Emission spectral changes (λ_{ex} = 313 nm) for a DMSO solution of $[\mathbf{1}](PF_6)_2$ upon addition of a solution of Br^- (from tetrabutylammonium bromide); a) $[\mathbf{1}](PF_6)_2$ in DMSO (0.2 mM) (b) the fluorescence emission spectra of the same solution of $[\mathbf{1}](PF_6)_2$ diluted in DMSO containing between 0 and 550 molar equivalents of Br^- per Au ion.

X-ray Absorption Spectroscopy

X-ray absorbtion spectra were recorded at the Au L_3-edge for $[\mathbf{1}]^{2+}$ in the presence and absence of Br^- ions. Fig. 3 shows the X-ray absorption near edge spectra (XANES) of $[\mathbf{1}](PF_6)_2$ recorded from a DMSO solution. The energy of the Au L_3-edge for $[\mathbf{1}](PF_6)_2$ is 11920.2 eV (first derivative), while the addition of Br^- ions (Au:Br 1:1) caused a significant negative shift in the edge energy by 3 eV, to 11917.2 eV. The X-ray absorption edge energy is sensitive to the coordination environment of the metal, including donor strength and the number of ligands, where strongly electron donating ligands increase electron density at the

metal centre causing a decrease in the edge energy.[24] The decrease in the edge energy observed here, supports the notion that Br^- associates directly with Au atoms, and the increase in effective electron density on the Au atoms causes a decrease in the X-ray energy required to eject a photoelectron from the core that gives rise to the edge position.

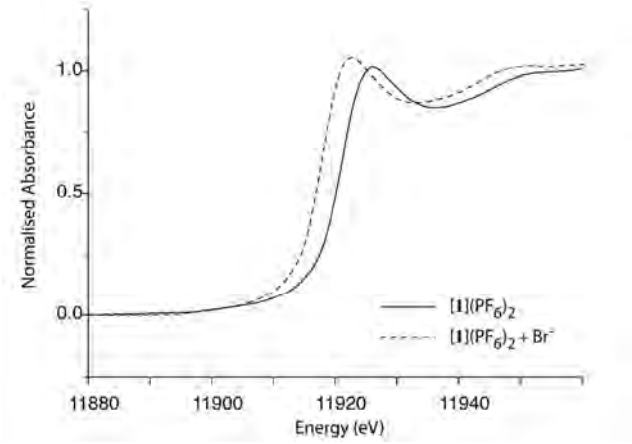

Fig. 3 XANES (Au-L_3) spectra of [**1**]$(PF_6)_2$ in DMSO (20 mM), before and after the addition of an equimolar amount of bromide ions (Br : Au = 1) showing the shift in edge energy (3 eV).

EXAFS Analysis

To obtain structural information on the adduct formed between the cation $[\mathbf{1}]^{2+}$ and Br^- ions, the extended X-ray absorption fine structural (EXAFS) region of the XAS spectrum for [**1**]$(PF_6)_2$ in DMSO was modelled. A simplified model of the local Au(I) environment was constructed using structural information from the crystal structure of [**1**]Br_2.[7] The model included the dinuclear Au(I) core and the coordinated five-membered NHC groups on the absorbing Au(I) atom. The starting geometry for the EXAFS model used Au-carbene bond lengths and Au•••Au distance of 2.03 Å and 2.93 Å, respectively. An excellent fit was obtained from multiple scattering analysis of the EXAFS data (R = 16.71%), and the results are summarised in Table 1. The observed and calculated EXAFS, $\chi(k) \times k^3$, the corresponding Fourier transforms, the residuals, $\Delta[\chi(k) \times k^3]$, and the window functions used in the Fourier filter for [**1**]$(PF_6)_2$ in DMSO, are shown in Fig. 4. The EXAFS-derived model structure obtained after fitting the EXAFS data is shown in Fig. 5. The fitted values for the Au-carbene distance and Au•••Au distance were 2.03 and 3.02 Å, respectively. The paths and importance factors for this fit are contained in Tables S1 and S2 (Supporting Information).

Table 1 Summary of MS analysis of the EXAFS of [**1**]$(PF_6)_2$ in DMSO at 13K. The probable errors in the EXAFS-derived bond lengths for the MS model are given in the brackets ().

	Au-shell distances (Å)		Debye-Waller Factors, σ^2, (Å^2)				
	C(1/2)	Au(3)	C(1/2)	Au(3)	E_0	S_0^2	R (%)
MS model	2.03(0.02)	3.02(0.02)	0.0011	0.0013	-1.68	0.89	16.71
Crystal[7]	2.03	2.9209					

Consistent with the fluoresence studies (above), we envisaged that the Br^- ion would bind to the Au(I) atom on the axis defined by the Au•••Au interaction, with a T-shaped geometry relative to the NHC donor groups, where the Br^- ions would lie in the most sterically unhindered position. Due to possible partial occupancy of the Br^- position, resulting from the concentration-dependent equilibrium, the EXAFS data was most appropriately modelled using single scattering (SS) analysis.

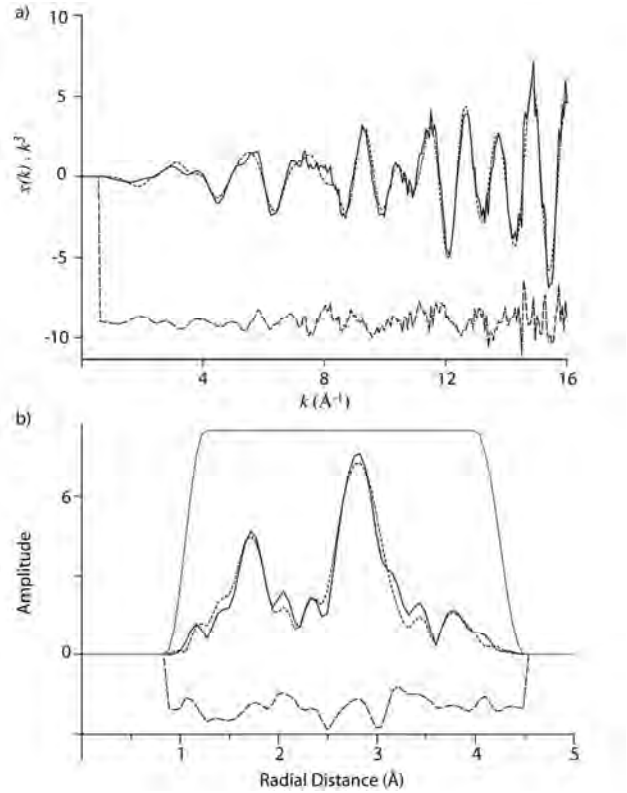

Fig. 4 (a) EXAFS and (b) Fourier transform amplitude of EXAFS of [**1**]$(PF_6)_2$ at 13 K: observed (solid line), calculated from MS model (dotted line), residual (dashed line), and the window used in Fourier filter (R = 16.71%).

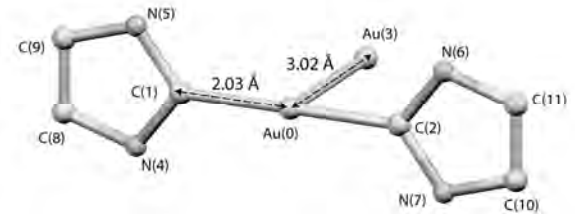

Fig. 5 EXAFS derived molecular structure of the dinuclear core of [**1**]$(PF_6)_2$ in DMSO at 13 K, using the MS input model (R = 16.71%).

A summary of SS results is provided in Table 2. A SS model based on two carbon (i.e. the carbenes) shells at 2.0 Å, and one gold shell at 3.0 Å was employed. The best fit for the EXAFS data was obtained for SS model **4** (Table 2, R = 26.22 %). This model included two partially occupied bromine shells (starting occupancy = 0.5). The distances of these partially occupied bromine shells from the Au absorber were refined, with the initial values being 3.0 Å and 4.0 Å from the absorber, respectively. The observed and calculated EXAFS, $\chi(k) \times k^3$, the corresponding

Table 2 Variations to SS input model on single-scattering fitting of $[\mathbf{1}]^{2+}$ in DMSO after the addition of Br^- ions. σ^2 = mean displacement factor, N = occupancy. Restraints and constraints are shown below the table.

	Au-shell distances, R_i, (Å) Debye-Waller Factors, σ^2, (Å^2)				Occupancy, N_i				
	C	Au	Br(1)	Br(2)	Br(1)	Br(2)	E_0	S_0^2	R(%)
Starting model – SS	2 0.004	3 0.004					-2	0.9	
1.^{SS}Fitted Results	1.97 0.0020	2.97 0.0020					-20.15	0.91	44.54
2.^{SS}Add Bromine at 3.0 Å†‡	1.97 0.0021	2.98 0.0026	2.94 0.0046				-18.21	0.9	34.96
3.^{SS}Add Bromine at 4.0 Å†‡	1.97 0.0019	2.98 0.0019	3.9 0.0034				-20.13	0.9	41.77
4.^{SS}Add Bromine at 3.0 and 4.0 Å†‡§	1.97 0.0021	2.99 0.0027	2.93 0.0010	3.91 0.0010	0.41	0.43	-18.94	0.9	26.22
5.^{SS}Add Bromine at 3.0 and 4.0 Å$^{\dagger\ddagger\S\square}$	1.97 0.0021	2.99 0.0028	2.95 0.0016	3.91 0.0010	0.52	0.48	-17.95	0.9	26.67

$^a N_{(C)} = 2$, $N_{(Au)} = 1$; $^\dagger S_0^2 \sim= 0.9\{0.1\}$, $E_0(0) > -20\{1\}$, $0.02\{0.001\} > \sigma^2_i > 0.001\{0.005\}$ (where i is shell number); $^\ddagger N_{(Br1)} = 1$, $\sigma^2_{(Br1)} = 0.004$; $^\S N_{(Br1)} = 0.5$, $N_{(Br2)} = 0.5$, $\sigma^2_{(Br2)} = 0.004$; $^\square N_{(Br1)} + N_{(Br2)} \sim= 1\{0.01\}$.

Fourier transforms, the residuals, $\Delta[\chi(k) \times k^3]$, and the window functions used in the Fourier filter for $[\mathbf{1}](PF_6)_2$ in DMSO after the addition of Br^- ions, are shown in Fig. 6. The final refined values from the SS analysis gave Au-carbene and Au•••Au distances of 1.97 and 2.99 Å, respectively. The occupancies of the two bromide shells refined to 0.41 and 0.43 and the final refined values for the Au-bromine distances were 2.98 and 3.9 Å, respectively. These results indicate that when bound to the Au(I) atoms, the Br^- ions occupy two sites, each with a refined occupancy of ~ 0.4. Restraining the occupancies to ~ 1 (SS model **5**, Table 2, R = 26.67 %) afforded no better fit to the data and a slight increase in the residual.

Similar results were obtained from the SS analysis of the EXAFS for a solid sample of $[\mathbf{1}]Br_2$, a summary of which is provided in Table 3 .The observed and calculated EXAFS, $\chi(k) \times k^3$, the corresponding Fourier transforms, the residuals, $\Delta[\chi(k) \times k^3]$, and the window functions used in the Fourier filter for a solid sample of $[\mathbf{1}]Br_2$, are shown in Fig. 7. These results are consistent with the solution XAS studies, showing that Br^- ions interact with the Au(I) atoms at two sites (~ 2.9 and 3.9 Å), both partially occupied.

Taken together the luminescence, XANES and EXAFS studied support the notion that the dinuclear complex $[\mathbf{1}](PF_6)_2$ forms an association complex with Br^- ions in solution. Previous studies have shown that the identity of coordinating halides (i.e. Cl^-, Br^-, I^-) can have a profound effect on the degree of aurophilicity.[25] Here, coordination of an anion (which is electron donating and/or easily polariseable) to the Au(I) atoms, causes an increase in the nephalauxetic effect for the Au(I) atoms. The nephalauxetic effect is characterised by radial orbital expansion (already significant for Au(I) due to relativistic effects),[26] and a decrease in the positive charge on the Au(I) centres, thereby favouring weak (aurophilic) interactions between the Au(I) atoms.

Furthermore, crystallographic studies have demonstrated that the association of Br^- ions with dinuclear Au(I) phosphine complexes occurs in the solid state, with typical Au(I)•••Br distances being ~ 3.52 Å for $[Au_2(dmpm)_2]Br_2.2H_2O$ (dmpm = is bis(dimethylphosphino)methane), and 3.08 and 3.11 Å for $[Au_2(dmpe)_2].Br_2.1.5H_2O$ (dmpe = bis(dimethy1phosphino) ethane), and that the equilibrium association between the free Au complex and the halide bound complex results in significant changes in the emission spectral properties.[10]

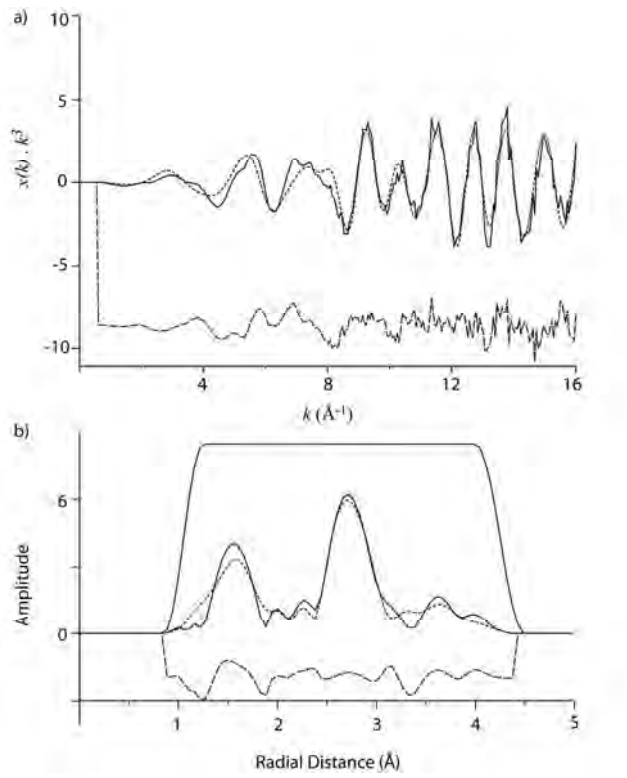

Fig. 6 (a) EXAFS and (b) Fourier transform amplitude of EXAFS of $[\mathbf{1}](PF_6)_2$ after the addition of bromide ions, at 13 K in DMSO solution: observed (solid line), calculated from SS model **4** (dotted line), residual (dashed line), and the window used in Fourier filter (R = 26.22%).

Table 3 Variations to SS input model on single-scattering fitting of a solid sample of [**1**]Br_2 in DMSO. σ^2 = mean displacement factor, N = occupancy. Restraints and constraints are shown below the table.

	Au-shell distances, R_i, (Å) Debye-Waller Factors, σ^2, (Å^2)				Occupancy, N_i				
	C	Au	Br(1)	Br(2)	Br(1)	Br(2)	E_0	S_0^2	R(%)
Starting model – SS	2 0.004	3 0.004					-2	0.90	
1.[SS]Fitted Results	1.96 0.0024	2.97 0.0020					-20.01	0.91	30.88
2.[SS]Add Bromine at 3.0 Å[†‡]	1.97 0.0025	2.99 0.0021	2.95 0.0087				-15.1	0.90	29.17
3.[SS]Add Bromine at 4.0 Å[†‡]	1.96 0.0024	2.99 0.0020	3.89 0.0081				-20.00	0.91	30.07
4.[SS]Add Bromine at 3.0 and 4.0 Å[†‡§]	1.97 0.0026	3.01 0.0023	2.95 0.001	3.93 0.001	0.23	0.27	-14.29	0.9	23.02
5.[SS]Add Bromine at 3.0 and 4.0 Å[†‡§¤]	1.97 0.0026	3.01 0.0025	2.96 0.0010	3.93 0.0047	0.27	0.73	-13.05	0.9	24.61

[a]$N_{(C)} = 2$, $N_{(Au)} = 1$; [†]$S_0^2 \sim= 0.9\{0.1\}$, $E_0(0) > -20\{1\}$, $0.02\{0.001\} > \sigma^2_i > 0.001\{0.005\}$ (where i is shell number); [‡]$N_{(Br1)} = 1$, $\sigma^2_{(Br1)} = 0.004$; [§] $N_{(Br1)} = 0.5$, $N_{(Br2)} = 0.5$, $\sigma^2_{(Br2)} = 0.004$; [¤] $N_{(Br1)} + N_{(Br2)} \sim= 1\{0.01\}$.

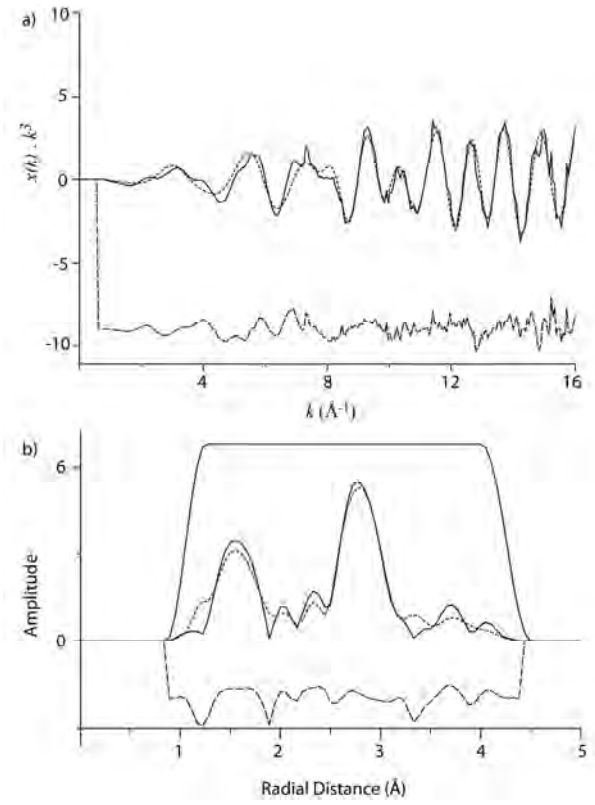

Fig. 7 (a) EXAFS and (b) Fourier transform amplitude of EXAFS of a solid sample of [**1**]Br_2 at 13 K: observed (solid line), calculated from SS model **4** (dotted line), residual (dashed line), and the window used in Fourier filter (R = 23.02%).

Conclusion

The concentration dependent changes in the emission spectra for the dinuclear complex $[\mathbf{1}]^{2+}$ induced by the addition of Br^- ions strongly indicates that an association complex is formed in solution. Consistent with previous reports on other dinuclear Au(I) complexes, the association complex is likely to arise as a result of an electrostatic interaction between the linear two-coordinate Au(I) atoms and the Br^- ions, where the Au(I) ions are essentially three-coordinate.

The decrease in the XANES Au L_3-edge for $[\mathbf{1}]^{2+}$ further supports this notion, with a decrease in the ionisation energy associated with coordination of Br^- to the Au(I) centres of $[\mathbf{1}]^{2+}$. A good fit was obtained for the multiple scattering analysis of the EXAFS for a simplified model of the Au(I) coordination environment of [**1**]$(PF_6)_2$. Single scattering analysis of [**1**]$(PF_6)_2$ with the addition of Br^- ions provide a model for the complex with two partially occupied Br^- sites with Au-Br distances of 2.93 and 3.91 Å, respectively.

The dependence of the emission wavelength on the halide ion concentration is significant in light of the previously demonstrated application of these dinuclear Au(I) NHC complexes as luminescent probes in live cell imaging studies.[7] It is well established that Cl^- ion concentration can vary significantly between cell types, in particular in disease states such as cancer, where $[Cl^-]$ can ranges from 12 to 55 mM.[27] We reason that appropriately designed dinuclear Au(I) complexes may be useful as cellular probes of Cl^- ion concentration and this potential application is currently being explored in our laboratory.

Acknowledgements

This research was undertaken at the Australian National Beamline Facility at the Photon Factory in Japan, operated by the Australian Synchrotron. We acknowledge the Australian Research Council for financial support and the High Energy Accelerator Research Organisation (KEK) in Tsukuba, Japan, for operations support. We acknowledge travel funding provided by the International Synchrotron Access Program (ISAP) managed by the Australian Synchrotron and funded by the Australian Government. The authors thank Associate Professor Murray Baker for useful discussions on the synthesis and characterisation of $[\mathbf{1}]^{2+}$, and Professor Peter Lay for helpful suggestions regarding modelling of the EXAFS data.

References

1. H. Schmidbaur, *Gold Bull.*, 1990, **23**, 11-21.
2. H. Schmidbaur, *Chem. Soc. Rev.*, 1995, **24**, 391-400; H. Schmidbaur, *Gold Bull.*, 2000, **33**, 3-10.

3. M. Saitoh, A. L. Balch, J. Yuasa and T. Kawai, *Inorg. Chem.*, 2010, **49**, 7129-7134.
4. A. Vogler and H. Kunkely, *Coord. Chem. Rev.*, 2001, **219-221**, 489-507; V. W.-W. Yam and E. C.-C. Cheng, *Top. Curr. Chem.*, 2007, **281**, 269-309; V. W.-W. Yam and E. C.-C. Cheng, *Chem. Soc. Rev.*, 2008, **37**, 1806-1813; E. R. T. Tiekink and J.-G. Kang, *Coord. Chem. Rev.*, 2009, **253**, 1627-1648; M. Ferrer, A. Gutiérrez, L. Rodríguez, O. Rossell, J. C. Lima, M. Font-Bardia and X. Solans, *Eur. J. Inorg. Chem.*, 2008, 2899-2909; L. Rodríguez, M. Ferrer, R. Crehuet, J. Anglada and J. C. Lima, *Inorg. Chem.*, 2012, **51**, 7636-7641.
5. H. Schmidbaur and A. Schier, *Chem. Soc. Rev.*, 2012, **41**, 370-412.
6. P. J. Barnard, M. V. Baker, S. J. Berners-Price, B. W. Skelton and A. H. White, *Dalton Trans.*, 2004, 1034-1047.
7. P. J. Barnard, L. E. Wedlock, M. V. Baker, S. J. Berners-Price, D. A. Joyce, B. W. Skelton and J. H. Steer, *Angew. Chem., Int. Ed.*, 2006, **45**, 5966-5970.
8. W.-F. Fu, K.-C. Chan, K.-K. Cheung and C.-M. Che, *Chem.-Eur. J.*, 2001, **7**, 4656-4664.
9. W.-F. Fu, K.-C. Chan, V. M. Miskowski and C.-M. Che, *Angew. Chem., Int. Ed.*, 1999, **38**, 2783-2785.
10. H.-R. C. Jaw, M. M. Savas, R. D. Rogers and W. R. Mason, *Inorg. Chem.*, 1989, **28**, 1028-1037.
11. H.-X. Zhang and C.-M. Che, *Chem. Eur. J.*, 2001, **7**, 4887-4893.
12. C. Hemmert, R. Poteau, F. J.-B. dit Dominique, P. Ceroni, G. Bergamini and H. Gornitzka, *Eur. J. Inorg. Chem.*, 2012, 3892-3898.
13. E. J. Fernandez, J. M. Lopez-de-Luzuriaga, M. Monge, M. E. Olmos, R. C. Puelles, A. Laguna, A. A. Mohamed and J. P. Fackler, Jr., *Inorg. Chem.*, 2008, **47**, 8069-8076; M. A. Rawashdeh-Omary, M. A. Omary, H. H. Patterson and J. P. Fackler, Jr., *J. Am. Chem. Soc.*, 2001, **123**, 11237-11247; R. L. White-Morris, M. M. Olmstead and A. L. Balch, *J. Am. Chem. Soc.*, 2003, **125**, 1033-1040; R. L. White-Morris, M. M. Olmstead, F. Jiang, D. S. Tinti and A. L. Balch, *J. Am. Chem. Soc.*, 2002, **124**, 2327-2336.
14. C.-H. Li, S. C. F. Kui, I. H. T. Sham, S. S.-Y. Chui and C.-M. Che, *Eur. J. Inorg. Chem.*, 2008, 2421-2428.
15. K. H. Leung, D. L. Phillips, M.-C. Tse, C.-M. Che and V. M. Miskowski, *J. Am. Chem. Soc.*, 1999, **121**, 4799-4803.
16. H. de la Riva, A. Pintado-Alba, M. Nieuwenhuyzen, C. Hardacre and M. C. Lagunas, *Chem. Commun.*, 2005, 4970-4972.
17. A. Thompson, D. Attwood, E. Gullikson, M. Howells, K.-J. Kim, J. Kirz, J. Kortright, I. Lindau, P. Pianetta, A. Robinson, J. Scofield, J. Underwood, D. Vaughn, G. Williams and H. Winick, *X-Ray Data Booklet*, 3rd edn., Centre for X-Ray Optics and Advanced Light Source, Berkeley, 2009.
18. J. E. Penner-Hahn, *Coord. Chem. Rev.*, 1999, **190-192**, 1101-1123.
19. A. M. Rich, R. S. Armstrong, P. J. Ellis and P. A. Lay, *J. Am. Chem. Soc.*, 1998, **120**, 10827-10836.
20. P. J. Ellis and H. C. Freeman, *J. Synchrotron Radiat.*, 1995, **2**, 190-195.
21. J. J. Rehr, R. C. Albers and S. I. Zabinsky, *Phys. Rev. Lett.*, 1992, **69**, 3397-3400.
22. A. M. Rich, R. S. Armstrong, P. J. Ellis, H. C. Freeman and P. A. Lay, *Inorg. Chem.*, 1998, **37**, 5743-5753.
23. A. Levina, R. S. Armstrong and P. A. Lay, *Coord. Chem. Rev.*, 2005, **249**, 141-160.
24. R. A. Scott, in *Physical Methods in Bioinorganic Chemistry Spectroscopy and Magnetism*, ed. L. Que, University Science Books, Sausalito, CA, 2000, pp. 465-503.
25. S. M. Humphrey, H.-G. Mack, C. Redshaw, M. R. J. Elsegood, K. J. H. Young, H. A. Mayer and W. C. Kaska, *Dalton Trans.*, 2005, 439-446.
26. P. Schwerdtfeger, *Heteroatom Chem.*, 2002, **13**, 578-584.
27. M. Jennerwein and P. A. Andrews, *Drug Metab. Dispos.*, 1995, **23**, 178-184.

Bromide ion binding by a dinuclear gold(I) *N*-heterocyclic carbene complex: A spectrofluorescence and X-ray absorption spectroscopic study

Louise E. Wedlock, Jade B. Aitken, Susan J. Berners-Price and Peter J. Barnard

Electronic Supplementary Information

Contents

1. **Table S1**: Constraints and restraints used in the MS EXAFS analysis of 1.$(PF_6)_2$ in DMSO.
2. XFit Data Analysis – Determinacy, Goodness-of-Fit and Monte-Carlo Error Analysis
3. **Table S2**: Paths and importance factors from the analysis using MS model (Table 1), for the MS refinement of the EXAFS of **1**.$(PF_6)_2$.
4. ^{1}H NMR spectrum of [**1**]$(PF_6)_2$ in d_6-DMSO

Table S1 Constraints and restraints used in the MS EXAFS analysis of **1**.$(PF_6)_2$ in DMSO.

Mean displacement factor constraints (Å^2)	$\sigma^2_{(C1)} = \sigma^2_{(C2)}$ $\sigma^2_{(N4)} = \sigma^2_{(N5)} = \sigma^2_{(N6)} = \sigma^2_{(N7)}$ $\sigma^2_{(C8)} = \sigma^2_{(C9)} = \sigma^2_{(C10)} = \sigma^2_{(C11)}$
Mean displacement factor restraints (Å^2)	$\sigma^2_i > 0.0005$ {0.0001} where *i* is all shells $\sigma^2_i < 0.02$ {0.01} where *i* is all shells
Bond length restraints (Å)	C(1) – Au(0) ~= 2.03 {0.05} C(2) – Au(0) ~= 2.03 {0.05} C(1) – N(5) ~= 1.38 {0.05} C(5) – C(9) ~= 1.40 {0.05} C(8) – C(9) ~= 1.35 {0.05} C(8) – N(4) ~= 1.40 {0.05} N(4) – C(1) ~= 1.38 {0.05} C(2) – N(6) ~= 1.38 {0.05} N(6) – C(11) ~= 1.40 {0.05} C(10) – C(11) ~= 1.35 {0.05} C(10) – N(7) ~= 1.40 {0.05} N(7) – C(2) ~= 1.38 {0.05}
Bond angle restraints (º)	Au(0) – C(1) – N(5) ~= 127 {5} Au(0) – C(1) – N(4) ~= 127 {5} C(1) – N(5) – C(9) ~= 110 {5} N(5) – C(1) – N(4) ~= 106 {5} N(5) – C(9) – C(8) ~= 107 {5} C(9) – C(8) – N(4) ~= 107 {5} C(8) – N(4) – C(1) ~= 110 {5} Au(0) – C(2) – N(6) ~= 127 {5} Au(0) – C(2) – N(6) ~= 127 {5} C(2) – N(6) – C(11) – N(6) ~= 110 {5} N(6) – C(2) – N(7) ~= 106 {5} N(6) – C(11) – C(10) ~= 107 {5} C(11) – C(10) – N(7) ~= 107 {5} C(10) – N(7) – C(2) ~= 110 {5}
Symmetry restraints	*zi* = 0, where *i* is all shells except Au(3) *x*Au(3) = 0 *y*Au(3) = 0 *x*N(4) = *x*N(5) *x*N(6) = *x*N(7) *x*C(8) = *x*C(9) *x*C(10) = *x*C(11) *x*C(1) = -*x*C(2) *x*N(4) = -*x*N(7) *x*N(5) = -*x*N(6) *x*C(8) = -*x*C(10) *x*C(9) = -*x*(11) *y*C(1) = *y*C(2) *y*N(4) = -*y*N(5) *y*N(6) = -*y*N(7) *y*C(8) = -*y*C(9) *y*C(10) = -*y*C(11) *y*N(6) = *y*N(5) *y*N(7) = *y*N(4) *y*C(10) = *y*C(8) *y*C(11) = *y*C(9)
Occupancy (*N*) restraints	$N_i = 1$, where *i* is all shells

XFit Data Analysis – Determinacy, Goodness-of-Fit and Monte-Carlo Error Analysis

Determinacy

The number of parameters being fitted, p, compared to the number of independent information data points (independent points in the EXAFS plus the number of independent structural parameters), N_i, was calculated to give the degree of determinacy N_i/p. If this ratio is < 1, then the model is considered to be underdetermined and a unique fit is not possible. In all cases the ratio was > 1 and, hence, the models were overdetermined. The value of N_i is given by:[1]

$$N_i = 2(\Delta r)(\Delta k)/\pi + \Sigma[D(N\text{-}2)+1] \quad (1)$$

where D is the number of dimensions in which the refinement takes place and N is the number of atoms in the unit.[2]

Goodness-of-Fit (Residual)

The method of determining the goodness of fit was through an R value where R is given by:

$$R = (\chi^2/\chi^2_{calculated=0})^{1/2} \quad (2)$$

where χ^2 is the quantity minimized during the refinement and $\chi^2_{calculated=0}$ is the value of χ^2 when the calculated EXAFS is uniformly 0.[3] Residual R values of ≤ 20% were considered reasonable for MS models, and relatively high (>20%) values of R are explained by the exclusion of multiple-scattering contributions on the SS models.[2, 4]

Monte-Carlo Error Analysis

Monte Carlo analyses were conducted to estimate the rms deviations in final parameters arising from the noise in the data. Two consecutive sets of 16 × 16 Monte-Carlo cycles were calculated and the resulting rms errors were combined with systematic errors to determine the final error estimates. The probable errors in the Au-C and Au•••Au bond lengths were estimated as $[\sigma_r^2 + \sigma_s^2]^{1/2}$, where σ_r and σ_s represent contributions from the random and systematic errors, respectively. The random (statistical) errors due to noise in the data were estimated by Monte Carlo calculations,[3] and the systematic errors were assigned a conservative consensus value, 0.02 Å.[5]

The following applies to tables of multiple scattering pathways presented in the supporting information: [a]The number of legs represents the path travelled by the photoelectron originating from and returning to the XAFS absorber Au(0). [b]The total distance travelled by the photoelectron (R_{eff}) is twice the value of R_{as}. [c]The importance factor (given to 2 d.p.), represents the percent contribution of a path relative to the strongest path Au(0) → C(1) → Au(0), including contribution from the Debye-Waller Factors. All pathways have a maximum of 5 legs per MS pathway, curve and plane wave filters of 3% and 2%, respectively, $R_{eff} \leq 10$ Å.

Table S2 Paths and importance factors from MS analysis (Table 1), for the MS refinement of the EXAFS of **1**.$(PF_6)_2$.

Atoms in MS Pathway	Legs[a]	Deg	R_{as} (Å)[b]	Importance Factor[c]
Au(0) →C(1) →Au(0)	2	2	2.03	100.00%
Au(0) →Au(3) →Au(0)	2	1	3.02	20.45%
Au(0) →N(4) →Au(0)	2	4	3.06	100.00%
Au(0) →N(6) →C(2) →Au(0)	3	8	3.23	100.00%
Au(0) →C(2) →N(6) →C(2) →Au(0)	4	4	3.40	30.40%
Au(0) →C(2) →C(1) →Au(0)	3	2	4.06	17.00%
Au(0) →C(1) →Au(0) →C(2) →Au(0)	4	2	4.06	32.47%
Au(0) →C(1) →Au(0) →C(1) →Au(0)	4	2	4.06	9.57%
Au(0) →N(4) →N(5) →Au(0)	3	4	4.16	6.03%
Au(0) →C(10) →Au(0)	2	4	4.25	28.73%
Au(0) →C(9) →C(1) →Au(0)	3	8	4.28	64.64%
Au(0) →C(2) →N(6) →N(7) →Au(0)	4	8	4.33	21.17%
Au(0) →C(1) →C(9) →C(1)	3	4	4.30	42.92%
Au(0) →C(10) →N(7) →Au(0)	3	8	4.36	43.09%
Au(0) →N(4) →C(8) →C(1) →Au(0)	4	8	4.38	55.71%
Au(0) →N(7) →C(2) →N(7) →Au(0)	4	4	4.43	24.06%
Au(0) →N(5) →C(1) →N(4) →Au(0)	4	4	4.43	5.63%
Au(0) →C(1) →N(4) →N(5) →C(1) →Au(0)	5	4	4.50	11.14%
Au(0) →N(6) →C(11) →N(6) →Au(0)	4	4	4.46	22.57%
Au(0) →C(8) →N(4) →C(1) →Au(0)	4	8	4.53	39.22%
Au(0) →C(1) →C(9) →N(5) →C(1) →Au(0)	5	8	4.55	41.91%
Au(0) →C(1) →N(4) →C(1) →N(5) →Au(0)	5	8	4.60	12.52%
Au(0) →N(4) →C(1) →N(4) →C(1) →Au(0)	5	8	4.60	28.98%
Au(0) →N(5) →C(9) →N(5) →C(1) →Au(0)	5	8	4.63	36.46%
Au(0) →C(9) →N(4) →Au(0)	3	8	4.77	9.88%
Au(0) →C(2) →C(11) →N(7) →Au(0)	4	8	4.79	10.43%
Au(0) →N(7) →C(10) →N(6) →Au(0)	4	8	4.87	4.55%
Au(0) →C(9) →C(8) →Au(0)	3	4	4.92	5.45%
Au(0) →C(8) →N(5) →C(1) →Au(0)	4	8	4.94	11.53%
Au(0) →C(11) →C(10) →C(2) →Au(0)	4	8	4.95	13.32%

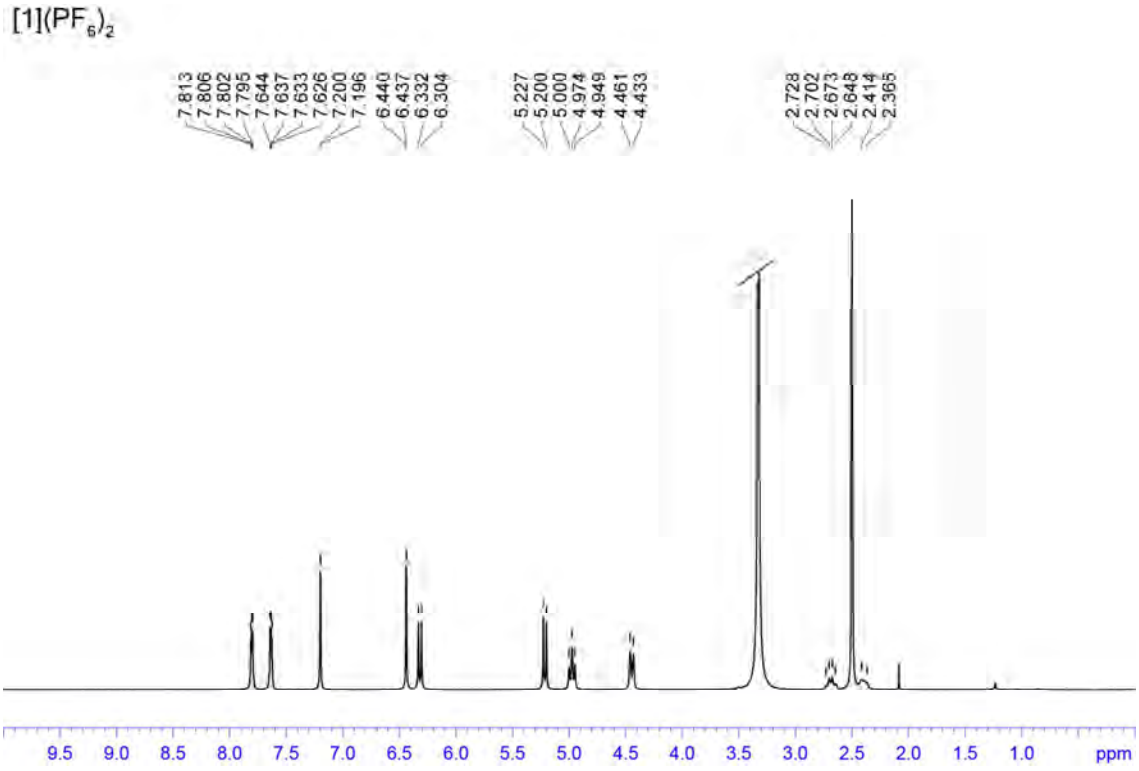

^{1}H NMR Spectrum of [**1**](PF$_6$)$_2$ in d6-DMSO

References

1. N. Binsted, R. W. Strange and S. S. Hasnain, *Biochemistry*, 1992, **31**, 12117-12125.
2. A. Levina, R. S. Armstrong and P. A. Lay, *Coord. Chem. Rev.*, 2005, **249**, 141-160.
3. P. J. Ellis and H. C. Freeman, *J. Synchrotron Radiat.*, 1995, **2**, 190-195.
4. A. M. Rich, R. S. Armstrong, P. J. Ellis, H. C. Freeman and P. A. Lay, *Inorg. Chem.*, 1998, **37**, 5743-5753.
5. S. J. Gurman, *J. Synchrotron Radiat.*, 1995, **2**, 56-63.

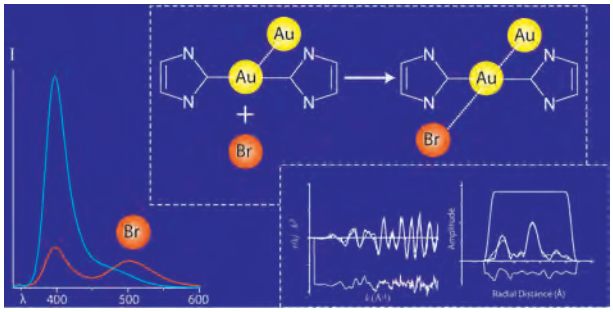

Evidence for a bromide association complex formation with a dinuclear luminescent Au(I) N-heterocyclic carbene complex in solution, revealed by spectrofluoresence and X-ray absorption spectroscopies.